NASA Technical Memorandum 102580

O_2 Reduction at the IFC Orbiter Fuel Cell O_2 Electrode

William L. Fielder and Joseph Singer
Lewis Research Center
Cleveland, Ohio

April 1990

NASA

O_2 REDUCTION AT THE IFC ORBITER FUEL CELL O_2 ELECTRODE

William L. Fielder and Joseph Singer
National Aeronautics and Space Administration
Lewis Research Center
Cleveland, Ohio 44135

SUMMARY

O_2 reduction Tafel data were obtained for the IFC Orbiter fuel cell O_2 electrode (Au-10%Pt catalyst) at temperatures between 24° and 81°C. BET measurements gave an electrode surface area of about 2040 cm^2 per cm^2 of geometric area. The Tafel data could be fitted to three straight line regions. For current densities less than 0.001 A/cm^2, the slope was essentially independent of temperature with a value of about 0.032 V/decade. Above 0.001 A/cm^2, the two regions, designated in the present study as the 0.04 and 0.12 V/decade regions, were temperature dependent. The "apparent" energies of activation for these two regions were about 9.3 and 6.5 kcal/mol, respectively.

Tafel data (1 atmosphere O_2) were extrapolated to 120°C for predicting changes in overpotential with increasing temperature. A mechanism is presented for O_2 reduction.

INTRODUCTION

Efficient electrical power systems are major requirements for space applications. For example, the International Fuel Cells Corporation (IFC) alkaline H_2-O_2 fuel cell is used as a primary energy source aboard the NASA Space Shuttle. While the energy density for the H_2-O_2 system is attractive, its voltage efficiency is less than 100 percent due primarily to the slower kinetics of the O_2 electrode.

Initially, IFC used Pt as an electrocatalyst for the O_2 electrode but the performance decayed with time due to the gradual dissolution of the Pt. IFC developed the Orbiter fuel cell electrode with an electrocatalyst of high surface area Au-10%Pt powder. Improved O_2 reduction performance and improved stability were reported for this electrode at 70°C (35% KOH, 1 atmosphere O_2) with Tafel slopes of 0.045 to 0.051 V/decade (refs. 1, 2). Endurance tests at 0.108 A/cm^2 at 60°C indicated that these electrodes were stable with minimal potential decay during a single cell endurance test of over 4000 hours (ref. 3).

Future space applications may require longer time operations at larger power densities. To satisfy these requirements, it may be necessary to operate the alkaline H_2-O_2 fuel cell at higher temperatures, pressures and current densities without significant degradation for 20,000 hours.

In the present study, O_2 reduction performance data is obtained for the IFC Orbiter O_2 electrode (1 atmosphere O_2) between 24° and 81°C. Electrode performance at higher temperatures are predicted from an extrapolation of the performance data. A mechanism for O_2 reduction is presented.

EXPERIMENTAL

Electrode Fabrication

An Orbiter O_2 electrode, with an electrocatalyst of Au-10%Pt, was obtained from IFC. It was reported that at least half of the Pt in the catalyst powder was alloyed in solid solution with Au. The surface area of the catalyst powder was 10-15 m^2/g. IFC mixed the catalyst powder with a Teflon[1] suspension and pressed the mixture onto a Au plated Ni wire screen current collector. The resulting "green" electrode was dried and "sintered" into a network by heating to produce a Teflon-bonded electrode. IFC optimized the Teflon-bonded electrode to allow sufficient access of O_2 gas to the catalyst-electrolyte interface without flooding the electrode (ref. 2).

Surface Area and Capacitance

A BET surface measurement of the electrode, using a Beta Scientific Automatic Surface Analyzer (Model 4200), gave a value of about 2040 cm^2 of BET surface area per cm^2 of geometric electrode area.

A cyclic voltammogram of the IFC electrode, obtained under N_2 gas at 1 mV/sec, is shown in figure 1.[2] Capacitances of the IFC electrode surface can be estimated from charging currents (under N_2) between 0.4 and 0.6 V where currents resulting from kinetic processes are small. This is illustrated in figure 2a (40°C) for a sweep at 1 mV/sec between 0.425 and 0.525 V. The capacitance can be calculated as follows: $C = 0.5 (i_a - i_c) / r$, where i_a and i_c are the anodic and cathodic currents expressed in mA, and r is the sweep rate in mV/sec. The cathodic current is expressed as a negative value. For example, anodic and cathodic currents of 0.259 and -0.315 mA were obtained at 0.475 V giving a value of about 0.227 farads per cm^2 of geometric area. Capacitances at various temperatures were also determined (figure 2b). These values are taken to be constant with temperature suggesting that the electrochemical surface area for the IFC electrode remains essentially unchanged between 24° and 81°C.

If the electrochemical surface area is assumed to be equal to the "BET" surface area (100% utilization of the electrocatalyst) and if the measured capacitance is assumed to be due to the double layer capacitance, the calculated value for the double layer capacitance is about 110 microfarad/cm^2 of electrochemical surface for the Au-10%Pt powder in the IFC electrode. This value is in reasonable agreement with the value of about 120 microfarad/cm^2 obtained for Au foil and the value of about 100 reported for Au (ref. 4).

Experimental Apparatus

A floating electrode half-cell apparatus was used for the electrochemical studies (ref. 5). A schematic is shown in figure 3. Coiled Au wire served as the counter electrode. One atmosphere of gaseous O_2 (or N_2) was passed into the half-cell apparatus through a presaturator cell which contained KOH at the same temperature and concentration as the half-cell.

---

1 Teflon is a trade mark of E. I. DuPont Co.

2 All potentials in the present study will refer to the reversible H_2 potential (RHE) unless otherwise stated.

This minimizes changes in KOH concentration by H_2O loss.

Galvanostatic current-potential measurements were obtained manually or by means of a computer-driven system. Both methods gave essentially the same results. For the computer-driven system, the potentiostat (EG&G Princeton Applied Research Model 173) was interfaced with a computer (Apple IIe) by means of a plug-in unit (EG&G Model 276). A computer program (EG&G Electrochemistry Program Volume I) was used to drive and control the potentiostat. For the manual runs, a EG&G Model 376 plug-in unit was used with the potentiostat.

IR polarizations were determined by means of an Electrosynthesis Corp. IR instrument (Model 800) in conjunction with a 7 volt Zener diode. Schematics are shown in figure 4. The IR instrument interrupts the current periodically for an interval of a few microseconds. The Zener diode limits the voltage rise to 7 V during the interruption.

Experimental Procedure

A Hg/HgO electrode served as the reference electrode. Its potential at 25°C is 0.926 V. The temperature coefficient for this Hg/HgO electrode, as seen in figure 5, is about -0.402 mV/°C as determined by comparisons of its potentials at various temperatures with a dynamic H_2 electrode.

A sample of the IFC electrode (1.266 cm^2 geometric area) was introduced into the half-cell as the working electrode with its catalyst side contacting the 30% KOH electrolyte surface. The electrode was then raised slightly to form a small meniscus at the electrode-electrolyte interface. Exact positioning of the electrode is not critical for determining IR corrected potentials. While the IR values may vary slightly with electrode positioning, the corresponding IR corrected potentials for a galvanostatic run still remains essentially constant for small meniscus heights.

Teflon-bonded electrodes often require cathodic preconditioning to minimize polarization. The IFC electrode was held cathodically at -0.9 A for about 1 hour. Then, prior to each series of runs, the electrode was held cathodically at -0.9 A for about 60 seconds.

Most galvanostatic runs were made without stirring since no appreciable changes in potential were observed with different stirring rates. Steady-state data were usually obtained after only a few seconds. This is illustrated in figure 6 for a typical run at 24°C: steady-state conditions were obtained within about 10 seconds for a cathodic run at -0.5 A and within about 30 seconds for a cathodic run at -0.001 A. Once steady-state conditions are obtained, the potential remains constant with time as illustrated by a cathodic run at -0.5 A for 1800 seconds (figure 6c).

IR potential corrections were obtained from plots of IR polarizations against currents as illustrated in figure 7 for a typical galvanostatic run.

RESULTS

O_2 reduction data for the IFC Orbiter O_2 electrode were obtained between

24°C and 81°C. Polarization potentials for each temperature were determined by subtracting the steady-state potentials (IR corrected) from the corresponding reversible O_2 electrode potentials (e.g. 1.230 V at 24°C). Polarization potentials, considered in the present study as having a positive sign, were plotted against the logs of the geometric current densities. The data for each temperature run could be fitted to three straight line regions.

For currents densities less than 0.001 A/cm^2, slopes of about 0.03 V/decade were obtained. This is illustrated in figure 8 for a run at 24°C where the data could be fitted to a line with a slope of 0.0326 V/decade. The resulting slopes and intercepts (i.e. polarization potentials at 1 A/cm^2) are listed in Table I. The slope is taken to be independent of temperature for this current density region giving an average value of 0.032 V/decade.

For currents densities greater than 0.001 A/cm2, the data for each temperature can be fitted to two straight line regions as shown in figures 9 and 10 for 24°C and 81°C, respectively. The lower current density region, designated in the present study as the 0.04 region, is illustrated in figure 9 at 24°C where the data between 0.0020 and 0.016 A/cm^2 can be fitted to a line with a slope of 0.0416 V/decade. The results are listed in Table II. The values for the slopes for this region increase with temperature. This increase in values for the slopes is illustrated in figure 11a where the slopes for this region are plotted against temperatures. In addition, the upper current limits for this 0.04 Tafel region (prior to higher slope region control) increase with temperature. For example, while 0.016 A/cm^2 is the upper limit at 24°C, 0.100 A/cm^2 is the upper current limit for the 0.04 region at 81°C.

A shorter straight line region with a larger slope is obtained for the higher currents (figures 9 and 10). This region, designated in the present study as the 0.12 V/decade region, is illustrated in figure 9 at 24°C where the data between 0.100 and 0.200 A/cm^2 can be fitted to a line with a slope of 0.120 V/decade. The results are listed in Table II. The values for the slopes for this region increase with temperature as illustrated in figure 11b where the slopes for this region are plotted against temperatures. In addition, the upper current limits (prior to non-kinetic control) for this region increase with temperature. For example, while the upper limit is about 0.200 A/cm^2 at 24°C, it is about 0.700 A/cm^2 at 81°C.

The slopes, as calculated from the least squares fits (figures 11a and 11b), are listed in Table III for the 0.04 and 0.12 regions. The intercepts and the corresponding geometric exchange current densities are also listed in Table III. The value of 2040 cm^2 of "BET" surface per cm^2 of geometric area is assumed for the electrochemical surface area. The corresponding "BET" exchange current densities are calculated and listed in Table III.

DISCUSSION

Electrode Performance

For currents less than 0.001 A/cm^2, the slope, as determined from polarization plots, was taken to be independent of temperature between 24° and 81°C with a value of about 0.032 V/decade.

Above 0.001 A/cm^2, two Tafel regions were obtained. Both slopes were temperature dependent in agreement with the Tafel expression where b represents the slope in V/decade: $b = 2.3\ R\ T\ /\ a\ F$. In the present study, the values for a are about 1.5 and 0.5 for the 0.04 and 0.12 regions, respectively.

The increase in the exchange current densities with temperatures, as seen in Table III, indicates that the O_2 reduction process at the IFC electrode surface is thermally activated. The "apparent" energy of activation for a reaction may be estimated by means of the following equation: $E_a^* = -2.3\ R\ [d\log i\ /\ d\log (1\ /\ T)]$ where E_a^* is the "apparent" energy of activation in cal/mol (ref. 6). An intermediate value of 0.280 V was assumed for the 0.04 region for each temperature. The values for log i at 0.280 V are calculated from the least square fit (Table III) and the results are plotted against 1/T in figure 12a. A least squares fit of this plot gives a slope of about -2040 K^{-1} for this 0.04 region with an "apparent" energy of activation of about 9.3 kcal/mol. A smaller slope of about -1420 K^{-1}, for an assumed potential of 0.360 V, is obtained from a similar type of plot for the 0.12 region (figure 12b). The "apparent" energy of activation for this region is about 6.5 kcal/mol. While values of 6.5 and 9.3 kcal/mol are relatively small, they are in reasonable agreement with a value of 4.71 kcal/mol reported for O_2 reduction at Pt electrodes in 0.3 M KOH (ref. 7).

The geometric current densities at 0.280 and 0.360 V for the 0.04 and 0.12 regions, respectively, were estimated for 120°C by extrapolating the least squares data of figures 12a and 12b. The resulting current densities are about 0.209 and 1.71 A/cm^2 for the two regions. Using extrapolated Tafel slope values of 0.0529 and 0.170 V/decade for the two regions, the Tafel plot for 120°C is shown in figure 13 as a solid line. This plot suggests that the upper current limit for the 0.04 region is about 1 A/cm^2 before inception of the 0.12 region. While data at 120°C for the 0.12 region are shown in figure 13 for current densities greater than 1 A/cm^2, this higher Tafel region for the IFC electrode may not be observable (or is very short) due to O_2 transfer limitations.

The data obtained at 81°C are also plotted in figure 13 as a dashed line. A comparison of the two plots illustrates the decrease in overpotential with increasing temperature. For example, the difference in overpotential at 0.1 A/cm^2 is about 0.03 V as indicated by the values of about 0.293 and 0.263 V, respectively, at 81° and 120°C.

O_2 Reduction Mechanisms

A Tafel slope of about 0.12 V/decade between 0.8 and 0.6 V, with a smaller slope above 0.8 V, was reported for O_2 reduction (in KOH) at Au surfaces. It was suggested that an O_2^- species was formed initially and that the formation of this species was the rate-controlling step for the 0.12 Tafel region. Electrochemical reduction of this species produces OH^- and O_2H^-.(ref. 8).

A second study reported a Tafel region with a slope of about 0.04 V/decade at smaller currents in addition to the 0.12 region. This study proposed that O_2 is electrochemically reduced to produce an O_2H intermediate and that the rate-controlling step for this 0.04 region is the electrochemical

reduction of this intermediate to produce O_2H^- (ref. 9).

Electrochemical reduction of O_2H^- to produce OH^- is influenced strongly by the crystal orientation of the Au surface. For example, O_2H^- is electrochemically reduced at moderate potentials at (100) Au (ref. 10) but not at the (110) or (111) orientations (ref. 11).

Even though O_2 is not significantly electrochemically reduced at (110) or (111) Au at moderate potentials, recycling of O_2 results in an apparent electron transfer of greater than 2. In addition to a value of 0.12 V/decade for the Tafel slope between 0.75 and 0.9 V, a recent study reported a smaller slope of about 0.035 on thin films of (111) Au above 0.9 V (ref. 12). It was suggested that some of the O_2H^-, produced from electrochemical reduction of O_2, subsequently decomposes catalytically to produce OH^- and O_2. Recycling of this O_2 produces additional O_2H^-. It was suggested that the currents for this 0.035 region are related to the amount of O_2H^- that is lost from the surface before being catalytically decomposed provided that the concentration of O_2 produced near the electrode surface is essentially equal to that in the bulk.

A more detailed reaction scheme for determining the kinetic parameters for O_2 reduction at single crystal Au electrodes was reported (refs. 13, 14 and 15). In simplified form, this scheme involves the following: O_2 is electrochemically reduced to O_2H^- by means of a 2-electron path through weakly adsorbed (physisorbed) species and to OH^- by means of a 4-electron path through strongly adsorbed (chemisorbed) species; some subsequent strong adsorption of this weakly adsorbed O_2H^- species (produced by the 2-electron path) produces OH^- by means of an "apparent" 4-electron process; some of the weakly adsorbed O_2H^- diffuses into the bulk but some of it decomposes catalytically to produce OH^- and O_2; recycling of this O_2 produces additional O_2H^-. Thus, the overall electron path may range between 2 and 4.

Anodic adsorption of oxy species at the IFC electrode surface starts at about 0.8 V as shown in figure 1. This is in agreement with cyclic voltammograms for (100) Au which shows anodic adsorption at about 0.8 V (ref. 10). Adsorption at (110) and (111) Au occurs at higher potentials (ref. 11). Other factors, however, suggest that the amount of (100) Au in the IFC Au-10%Pt electrode is small or insignificant. First, (111) Au is the more stable orientation as indicated by the formation of (111) Au after vapor deposition (ref. 12). Second, an alternate explanation for the observed adsorption at about 0.8 V for the IFC electrode may be the presence of free Pt which also shows adsorption in this region. Free Pt is assumed to be present in the IFC electrode as indicated by the following: some Pt remains unalloyed with Au (ref. 2); and H_2 adsorption-desorption peaks are observed between 0.1 and 0.3 V (figure 1). While a definitive determination of the Au orientation in the IFC electrode can not be made at present, it is assumed that the (111) Au predominates.

A combination of the processes proposed in the literature is presented in the present study to account for the three Tafel slope regions observed for O_2 reduction at the IFC electrode surface. In the following equations, the subscripts A and B represent species which are weakly adsorbed at the surface and or in the bulk, respectively:

$$O_{2,B} \quad --- \quad O_{2,A} \qquad (1)$$

$$O_{2,A} + e^- \quad --- \quad O_{2,A}^- \qquad (2)$$

$$O_{2,A}^- + HOH + e^- \quad --- \quad O_2H_{,A}^- + OH^- \qquad (3)$$

$$O_2H_{,A}^- \quad --- \quad 1/2O_2 + OH^- \qquad (4a)$$

$$O_2H_{,A}^- \quad --- \quad O_2H_{,B}^- \qquad (4b)$$

For the 0.032 V/decade region, observed at current densities less than 0.001 A/cm^2, some of the weakly adsorbed O_2H^-, produced in reaction 3 is catalytically decomposed, as indicated in reaction 4a, to produce O_2 which may be recycled in reaction 2. The rate for the process at the 0.032 V/decade region, as suggested in ref. 12, may be related to the rate of desorption and transfer of the $O_2H_{,A}^-$ species from the Au surface to the bulk.

For the 0.04 V/decade Tafel region, reaction 3 may become the rate-controlling step. The slopes obtained for this region are in agreement with a predicted value of about 0.0394 V/decade, with an a value of about 1.5, for a Tafel process at 25°C involving two consecutive 1-electron transfer steps (ref. 16).

At higher current densities, reaction 2 may become rate-controlling for the 0.12 V/decade Tafel region. The slopes, obtained for this region, are in agreement with a predicted value of 0.118 V/decade, with an a value of 0.5, for a Tafel process at 25°C involving one 1-electron transfer step.

REFERENCE

1. Freed, M.S.; and Lawrance, R.J.: Development of Gold Alloy Catalyst Cathode for Alkaline Electrolyte Fuel Cells. 147th Meeting Electrochemical Society, Toronto, Canada, May 15, 1975.

2. Martin, R.E.; and Manzo, M.A.: Alkaline Fuel Cell Performance Investigation. NASA TM-100937, 1988.

3. Martin, R.E.: Advanced Technology Light Weight Fuel Cell Program. NASA CR-159807, March 4, 1980.

4. Chaffins, S.A.; Srinivasan, V.S.; and Singer, J.: Electrocatalytic Reduction of Oxygen on Modified Oxide Surfaces, NASA TM-101333, 1988.

5. Giner, J.; and Smith, S.: A Simple Method for Measuring Polarization of Hydrophobic Gas Diffusion Electrodes. Electrochem. Tech., vol. 5, no. 1-2, Jan.-Feb. 1967, pp. 59-61.

6. Interfacial Electrochemistry. An Experimental Approach. Editors: Gileadi, E.; Kirowa-Eisner, E.; and Penciner, J.: Addison-Wesley Publishing Co. Inc., 1975, Reading, Massachusetts. p. 74.

7. Park, S-N.; Ho, S.; Aruliah, S.; Weber, M.F.; Ward, C.A.; Venter, R.D.; and Srinivasan, S.: Electrochemical Reduction of Oxygen at Platinum Electrodes in KOH Solutions - Temperature and Concentration Effects. J. Electrochem. Soc., vol. 133, 1986, pp. 1641-9.

8. Zurilla, R.W.; Sen, R.K.; and Yeager, E.: The Kinetics of the Oxygen Reduction Reaction on Gold in Alkaline Solution. J. Electrochem. Soc., vol. 125, 1978, pp. 1103-1109.

9. Damjanovic, A.; Genshaw, M.A.; and Bockris, J. O'M.: Hydrogen Peroxide Formation in Oxygen Reduction at Gold Electrodes. II. Alkaline Solution. J. Electroanal. Chem., vol. 15, 1967, pp. 173-180.

10. Adzic, R.R.; Markovic, N.M.; and Vesovic, V.B.: Structural Effects in Electrocatalysis. Oxygen Reduction on the Au(100) Single Crystal Electrode. J. Electroanal. Chem., vol. 165, 1984, pp. 105-120.

11. Markovic, N.M.; Adzic, R.R.; and Vesovic, V.B.: Structural Effects in Electrocatalysis. Oxygen Reduction on the Gold Single Crystal Electrodes with (110) and (111) Orientations. J. Electroanal. Chem., vol. 165, 1984, pp. 121-133.

12. Paliteiro, C.; Hamnett, A.; and Goodenough, J.B.: The Electroreduction of Dioxygen on Thin Films of Gold in Alkaline Solution. J. Electroanal. Chem., vol. 234, 1987, pp. 193-211.

13. Anastasijevic, N.A.; Vesovic, V.; and Adzic, R.R.: Determination of the Kinetic Parameters of the Oxygen Reduction Reaction Using the Rotating Ring-Disk Electrode. Part I. Theory. J. Electroanal. Chem., vol. 229, 1987, pp. 305-316.

14. Anastasijevic, N.A.; Vesovic, V.; and Adzic, R.R.: Determination of the Kinetic Parameters of the Oxygen Reduction Reaction Using the Rotating Ring-Disk Electrode. Part II. Applications. J. Electroanal. Chem., vol. 229, 1987, pp. 317-325.

15. Adzic, R.R.; Strbac, S.; and Anastasijevic, N.: Electrocatalysis of Oxygen On Single Crystal Gold Electrodes. Materials Chem. and Phys., vol. 22, 1989, pp. 349-375.

16. Damjanovic, A.; Genshaw, M.A.; and Bockris, J.O'M.: The Mechanism of Oxygen Reduction at Platinum in Alkaline Solutions With Special Reference to H_2O_2. J. Electrochem. Soc., vol. 114, 1967, pp. 1107-1112.

TABLE I. - SLOPES AND INTERCEPTS FOR THE ORBITER IFC O_2 ELECTRODE AT LOWER CURRENT DENSITIES

Temperature, °C	Slope, V/decade	Intercept, V
24	0.0326	0.366
34	0.0312	0.351
48	0.0321	0.339
69	0.0330	0.326
81	0.0321	0.317

TABLE II. - SLOPES AND INTERCEPTS FOR THE ORBITER IFC O_2 ELECTRODE AT HIGHER CURRENT DENSITIES

Temperature, °C	Slope, V/decade	Intercept, V	Current Density Range (Geometric), A/cm^2
A. 0.04 Region			
24	0.0416	0.378	0.0020 to 0.016
34	0.0426	0.372	0.0020 to 0.020
48	0.0428	0.359	0.0020 to 0.025
69	0.0475	0.349	0.0040 to 0.050
81	0.0480	0.341	0.0060 to 0.100
B. 0.12 Region			
24	0.120	0.474	0.100 to 0.200
34	0.118	0.452	0.130 to 0.320
48	0.126	0.429	0.250 to 0.400
69	0.143	0.398	0.400 to 0.630
81	0.148	0.391	0.500 to 0.700

TABLE III. - POLARIZATION DATA ASSUMING LEAST SQUARES FIT

Temp., °C	Slope, V/decade	Intercept, V	Geometric Exchange Current Density, A/cm^2	"BET" Exchange Current Density, A/cm^2
A. 0.04 Region				
24	0.0412	0.377	7.07×10^{-10}	3.52×10^{-13}
34	0.0424	0.371	1.78×10^{-9}	8.72×10^{-13}
48	0.0441	0.361	6.52×10^{-9}	3.19×10^{-12}
69	0.0467	0.347	3.71×10^{-8}	1.82×10^{-11}
81	0.0481	0.341	8.14×10^{-8}	3.99×10^{-11}
B. 0.12 Region				
24	0.116	0.471	8.70×10^{-5}	4.27×10^{-8}
34	0.121	0.454	1.77×10^{-4}	8.68×10^{-8}
48	0.129	0.430	4.64×10^{-4}	2.28×10^{-7}
69	0.141	0.398	1.50×10^{-3}	7.38×10^{-7}
81	0.148	0.391	2.28×10^{-3}	1.12×10^{-6}

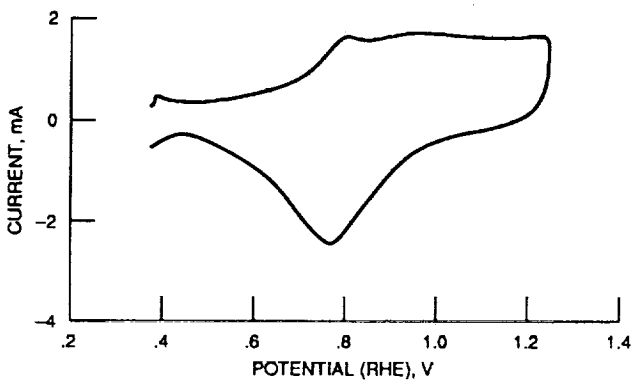

(a) Cycle from 0.39 to 1.25 volts.

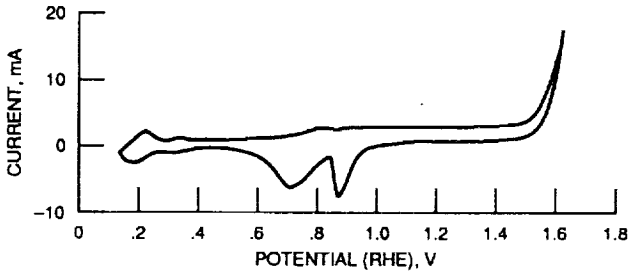

(b) Cycle from 0.15 to 1.58 volts.

Figure 1. - Cyclic voltammogram of IFC O_2 electrode at 1 mV/sec (24 °C, 1 atm N_2, 30 % KOH).

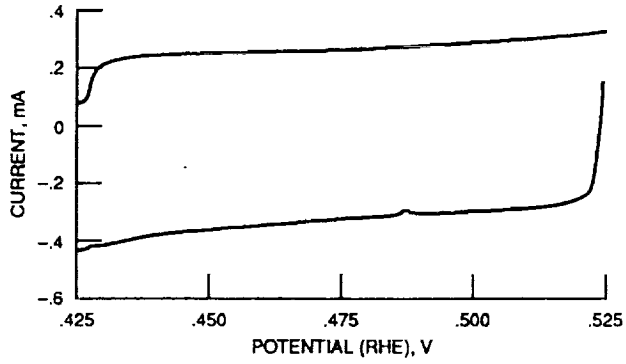

(a) Cyclic voltammogram (1 mV/sec, 40 °C).

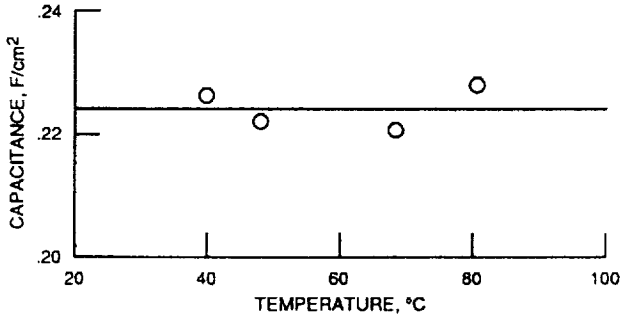

(b) Capacitance.

Figure 2. - Cyclic voltammogram and capacitance of IFC O_2 electrode (1 atm N_2, 30 % KOH).

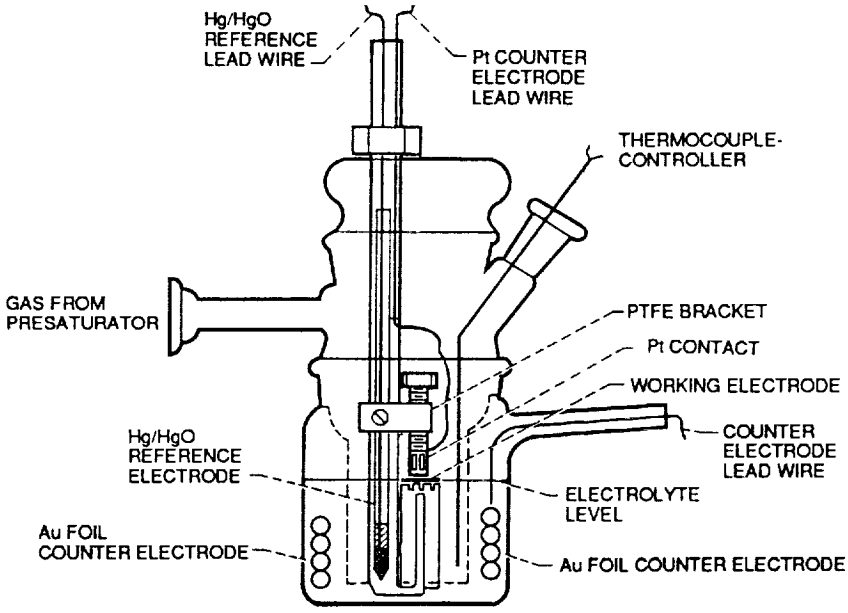

Figure 3. - Schematic of floating electrode half-cell apparatus.

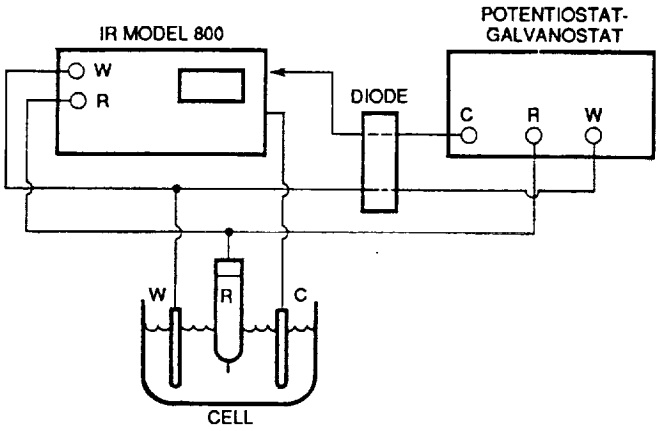

(a) Schematic for connection of cell and equipment to Electrosynthesis Corporation model 800 IR instrument.

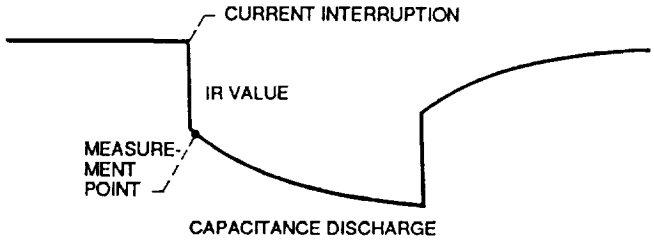

(b) Schematic of typical IR waveform for working electrode.

Figure 4. - IR polarization determination.

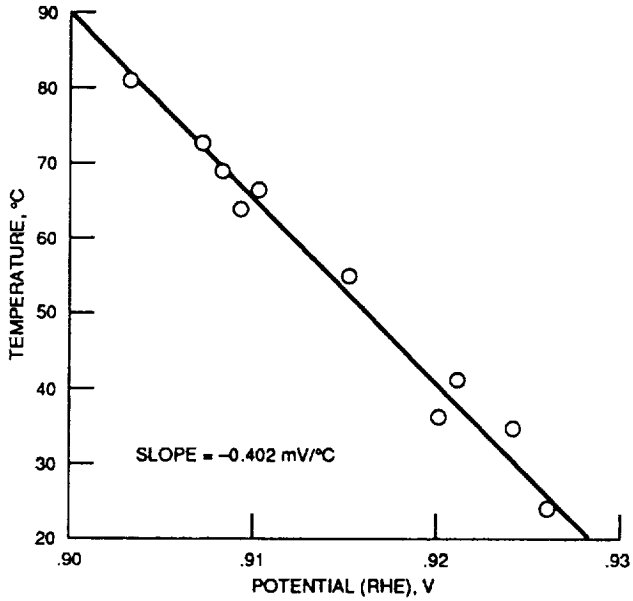

Figure 5. - Hg/HgO reference electrode potential with temperature (1 atm O_2, 30 % KOH).

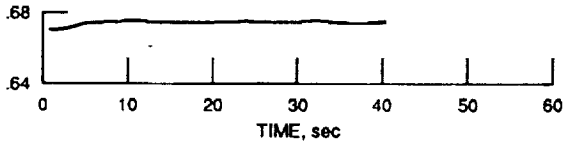

(a) Cathodic - 0.5 A.

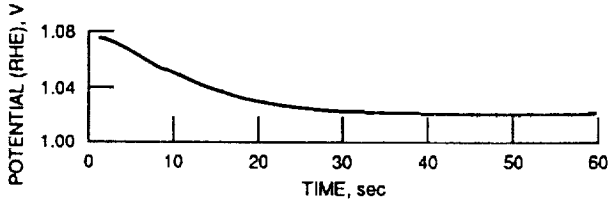

(b) Cathodic - 0.001 A.

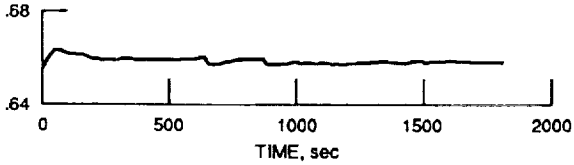

(c) Cathodic - 0.5 A.

Figure 6. - Galvanostatic O_2 reduction at IFC O_2 electrode (24 °C, 1 atm O_2, 30 % KOH).

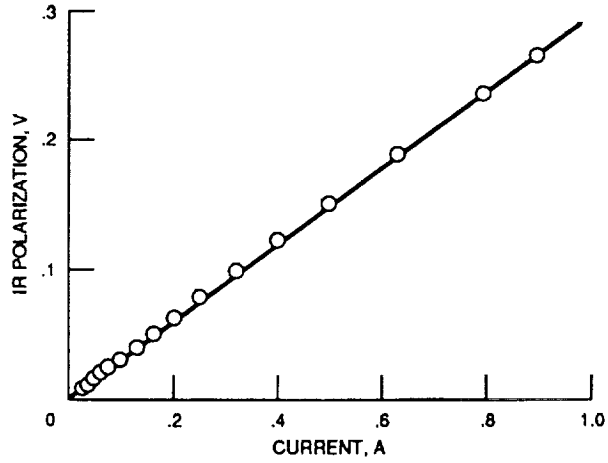

Figure 7. - IR polarization for galvanostatic O_2 reduction at IFC O_2 electrode (24 °C, 1 atm O_2, 30 % KOH).

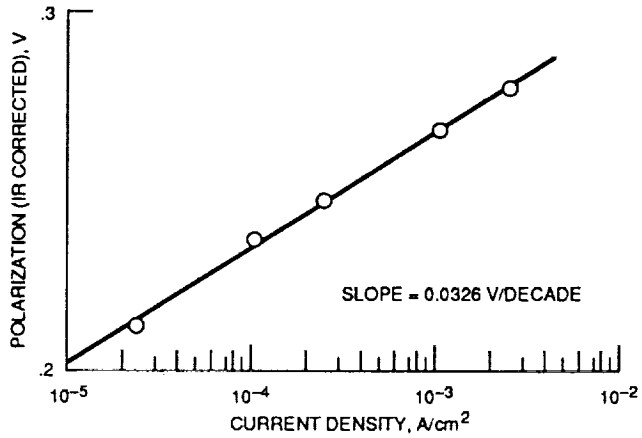

Figure 8. - Tafel plot of polarization against geometric current density for O_2 reduction at IFC O_2 electrode at 24 °C (1 atm O_2, 30 % KOH).

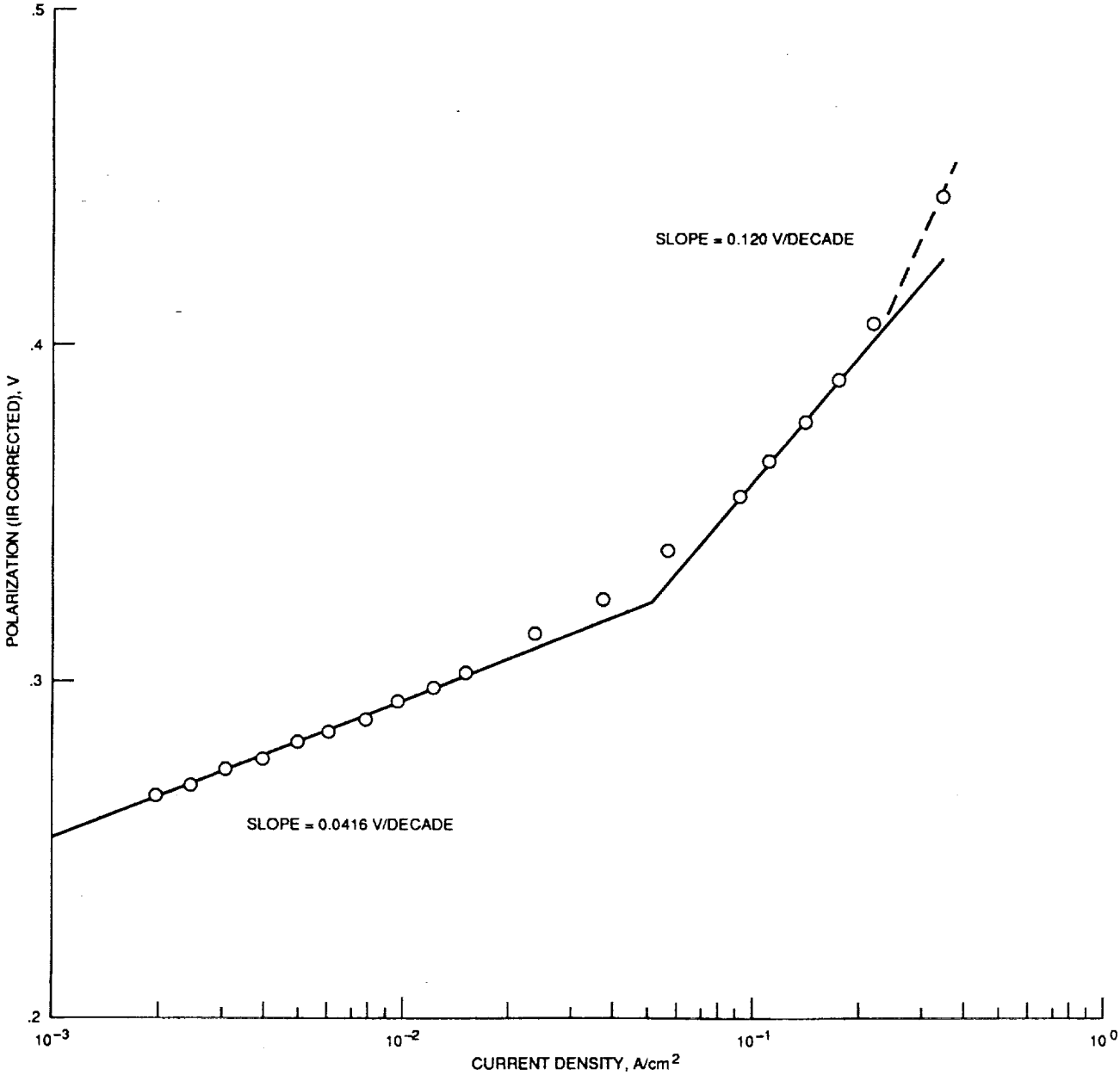

Figure 9. - Tafel plot of polarization against geometric current density for O_2 reduction at IFC O_2 electrode at 24 (1 atm O_2, 30 % KOH).

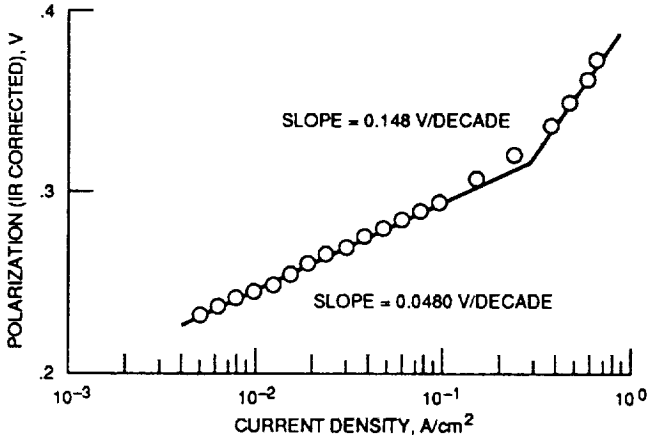

Figure 10. - Tafel plot of polarization against geometric current density for O_2 reduction at IFC O_2 electrode at 81 °C (1 atm O_2, 30 % KOH).

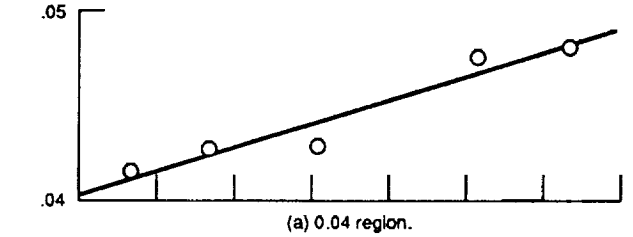

(a) 0.04 region.

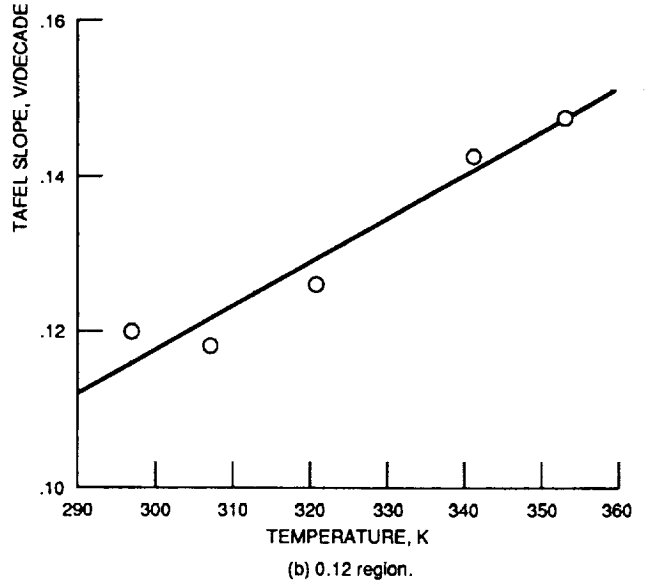

(b) 0.12 region.

Figure 11. - Plot ofTafel slope against temperature for O_2 reduction at IFC O_2 electrode (1 atm O_2, 30 % KOH).

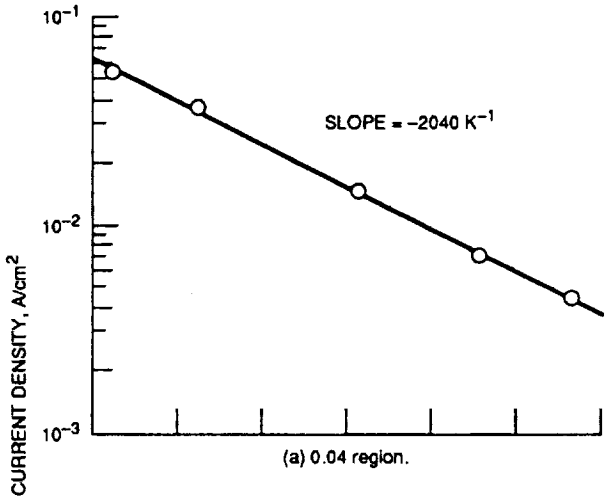

(a) 0.04 region.

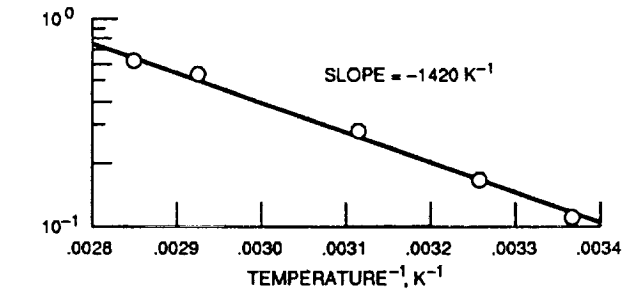

(b) 0.12 region.

Figure 12. - Plot of "apparent" exchange current density against reciprocal temperature for O_2 reduction at IFC O_2 electrode (1 atm O_2, 30 % KOH).

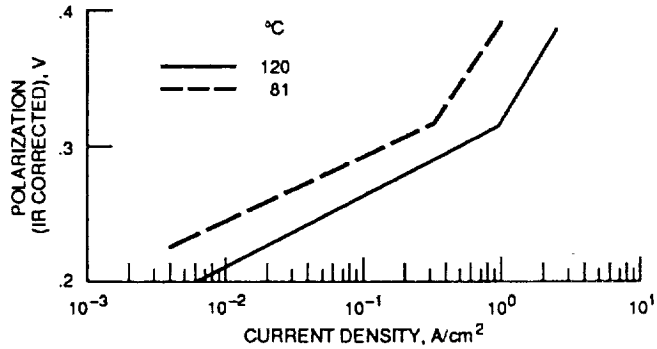

Figure 13. - Tafel plot of polarization against geometric current density for O_2 reduction at IFC O_2 electrode (1 atm O_2, 30 % KOH).

NASA
National Aeronautics and Space Administration

Report Documentation Page

1. Report No.	2. Government Accession No.	3. Recipient's Catalog No.
NASA TM-102580		

4. Title and Subtitle	5. Report Date
O_2 Reduction at the IFC Orbiter Fuel Cell O_2 Electrode	April 1990
	6. Performing Organization Code

7. Author(s)	8. Performing Organization Report No.
William L. Fielder and Joseph Singer	E-5411
	10. Work Unit No.
	506-41-21

9. Performing Organization Name and Address	11. Contract or Grant No.
National Aeronautics and Space Administration Lewis Research Center Cleveland, Ohio 44135-3191	
	13. Type of Report and Period Covered
	Technical Memorandum
12. Sponsoring Agency Name and Address	14. Sponsoring Agency Code
National Aeronautics and Space Administration Washington, D.C. 20546-0001	

15. Supplementary Notes

16. Abstract

O_2 reduction Tafel data were obtained for the IFC Orbiter fuel cell O_2 electrode (Au-10%Pt catalyst) at temperatures between 24 and 81 °C. BET measurements gave an electrode surface area of about 2040 cm^2 per cm^2 of geometric area. The Tafel data could be fitted to three straight line regions. For current densities less than 0.001 A/cm^2, the slope was essentially independent of temperature with a value of about 0.032 V/decade. Above 0.001 A/cm^2, the two regions, designated in the present study as the 0.04 and 0.12 V/decate regions, were temperature dependent. The "apparent" energies of activation for these two regions were about 9.3 and 6.5 kcal/mol, respectively. Tafel data (1 atmosphere O_2) were extrapolated to 120 °C for predicting changes in overpotential with increasing temperature. A mechanism is presented for O_2 reducution.

17. Key Words (Suggested by Author(s))	18. Distribution Statement
O_2 electrode Fuel cell O_2 reduction IFC electrode	Unclassified – Unlimited Subject Category 44

19. Security Classif. (of this report)	20. Security Classif. (of this page)	21. No. of pages	22. Price*
Unclassified	Unclassified	14	A03

NASA FORM 1626 OCT 86

*For sale by the National Technical Information Service, Springfield, Virginia 22161